Agonist efficiency estimated from concentration-response curves

Abbreviated title: agonist efficiency

Dinesh C. Indurthi and Anthony Auerbach[‡]

Department of Physiology and Biophysics

State University of New York at Buffalo

Buffalo NY 14214

[‡] Corresponding author: auerbach.anthony@gmail.com

Key words: acetylcholine receptor, nicotinic, affinity, efficacy, dose-response

Abstract

Concentration-response curves (CRCs) are characterized by a midpoint (EC_{50}) and a high-concentration asymptote (P_O^{max}) that relate to agonist affinity and efficacy. A third agonist attribute, efficiency, is the fraction of binding energy that is applied to the conformational change that activates the receptor. Here we show that agonist efficiency can be calculated from EC_{50} and P_O^{max}, and estimate the efficiencies of 17 agonists of adult muscle nicotinic acetylcholine receptors (AChRs). The distribution of efficiency values was bi-modal with means±s.d of 52±2% (n=11) and 41±3% (n=6). Efficiency is correlated inversely with the volume of the agonists' head-group. For 22 binding site mutations only αY190A affects significantly ACh efficiency, switching it from the high- to the low-efficiency population. If agonist efficiency is known, EC_{50} can be estimated from P_O^{max} and the receptor's level of constitutive activity can be calculated from a CRC.

Introduction

AChRs are members of the cys-loop, ligand-gated ion-channel receptor family that comprise GABA, glycine, and 5-HT_3 receptors. They are pentameric allosteric proteins that have agonist binding sites in the extracellular domain, ~60A° away from a narrow region of the pore in the transmembrane domain that regulates channel conductance (1). AChRs switch spontaneously between C(losed-channel) and O(pen-channel) conformations ('gating') to produce transient membrane currents (Fig. 1a). Agonists bind weakly to C versus strongly to O and increase receptor activity because the extra binding energy is used to facilitate the C→O transition (2). Here we are concerned with estimating the efficiency at which the agonist's chemical binding energy is converted to the mechanical work of the gating conformational change.

AChRs are the primary receptors at the neuromuscular synapse where they serve to initiate muscle membrane depolarization and contraction. They have two α1 subunits and one each of β, δ and either ε (adult) or γ (fetal). There are 2 neurotransmitter binding sites located at α–δ and α–ε/γ subunit interfaces (3). The presence of agonists at these sites increases the probability that the receptor will convert from the C to the O conformation and, hence, the probability that cations will enter and depolarize the muscle cell.

Agonists are typically characterized by an 'affinity' and an 'efficacy' (4). Affinity is a measure of how strongly the ligand binds to its target site and is the inverse of the equilibrium dissociation constant, either K_{dC} or K_{dO} (for binding to the site in its C or its O conformation). The concentration of agonist that produces a half-maximal response, EC_{50}, is proportional to K_{dC} (Eq. 3) and is sometimes called an 'apparent' affinity. Efficacy is the high-concentration asymptote of the CRC, or the maximum response elicited by the

ligand (P_O^{max}). Efficacy depends on the liganded gating equilibrium constant (Eq. 4) that is proportional to the equilibrium dissociation constant ratio, K_{dC}/K_{dO} (Eq. 2).

Recently, a third fundamental agonist attribute, efficiency (η; eta), was defined as the fraction of the agonist's chemical binding energy that is converted into the receptor's mechanical gating energy that moves the protein reversibly between the C-shape and the O-shape (5). As shown previously, and again below using a different approach, efficiency is a function of the binding energy ratio, $\log K_{dC}/\log K_{dO}$ (Eq. 5). Direct, independent measurements of these two equilibrium dissociation constants obtained by detailed modeling of single-channel currents indicated that at adult-type human AChR neurotransmitter binding sites ACh and 3 structurally-related agonists convert 52% of their binding energy to gating, whereas the frog toxin epibatidine and 3 related agonists convert only 39%. An efficiency value reflects the relationship between EC_{50} and efficacy. Given two agonists with the same EC_{50}, the higher-efficiency ligand has the greater efficacy.

Here we show how agonist efficiency can be estimated from EC_{50} and Po^{max}. We provide efficiency estimates from these CRC parameters for 17 agonists of mouse adult-type muscle AChRs, and show that knowledge of agonist efficiency simplifies and extends our understanding of drug action. If agonist efficiency is known, the apparent affinity (EC_{50}) can be calculated from the efficacy (Po^{max}).

Results

Estimating efficiency from CRC parameters.

Our first goal was to calculate agonist efficiency from EC_{50} and P_O^{max} using equations derived from Scheme 1 (Fig. 1). In order to ensure that the experimental measurements corresponded as closely as possible to the transitions in Scheme, we reduced the contribution from extraneous events such as channel block by the agonist, desensitization and modal activity (6), and constructed pseudo-macroscopic CRCs estimated from single-channel currents. Each CRC was a plot of the absolute open-channel probability (P_O, not normalized to a maximum value) versus [agonist], with the midpoint (EC_{50}), maximum (P_O^{max}) and slope (n_H) estimated by fitting to the empirical equation

$$P_O=P_O^{max}/(1+(EC_{50}/[\text{agonist}])^{n_H}). \qquad \text{Eq. 1}$$

From microscopic reversibility, Scheme 1 demands that the ratio of gating equilibrium constants (with/without agonists) is equal to the ratio of equilibrium dissociation constants (to C/to O) at two sites:

$$\frac{E_2}{E_0} = \left(\frac{K_{dC}}{K_{dO}}\right)^2 \qquad \text{Eq. 2}$$

where E_2 and E_0 are the diliganded and unliganded gating equilibrium constants. The exponent reflects the fact that in adult-type AChRs the 2 neurotransmitter binding-sites are approximately equivalent and independent (2). The diliganded gating equilibrium constant (that determines efficacy; see below) is equal to the constitutive gating equilibrium constant multiplied by the square of the fold-increase in agonist affinity that occurs within the C-to-O conformational change.

Constitutive and mono-liganded activities are both rare, so in wild-type (wt) AChRs the only route that generates a significant amount of current is the linear path

shown in bold in Fig. 1. Transitions between these 4 states determine P_O and, hence, the experimental values of EC_{50} and P_O^{max}. For activation by this pathway, EC_{50} depends on both binding (to C) and gating equilibrium constants, but P_O^{max} depends only on the diliganded gating equilibrium constant (7),

$$EC_{50} = \frac{K_{dC}\sqrt{E_2+2}}{E_2+1} \qquad \text{Eq. 3}$$

$$P_O^{max} = \frac{1}{1+\frac{1}{E_2}} \qquad \text{Eq. 4}$$

Fig. 1

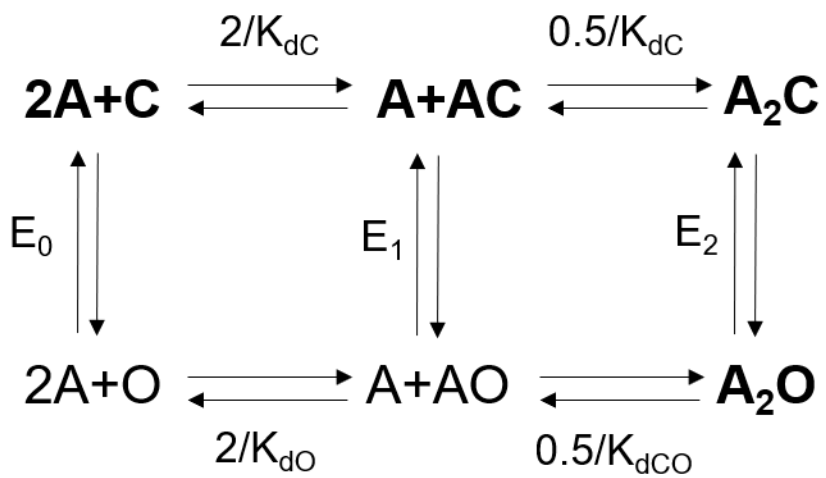

Figure 1. Cyclic activation of receptors (Scheme 1). AChRs switch spontaneously between resting (C) and active (O) conformations. A, agonist. Horizontal arrows, binding and vertical arrows, gating. Equilibrium constants: E_n, gating with n bound agonists; K_{dC} and K_{dO}, dissociation constants to C (low affinity) and to O (high affinity). Rate and equilibrium constants for all steps have been measured experimentally in adult-type endplate AChRs that have two approximately equivalent and independent neurotransmitter binding sites. From microscopic reversibility, $E_2/E_0=(K_{dC}/K_{dO})^2$ (Eq. 2). Agonists increase activity above the baseline level because they bind more-strongly to O, with the extra binding energy facilitating the spontaneous channel-opening transition. Bold, the main physiological activation pathway.

Agonist efficiency (η) was calculated from EC_{50} and P_O^{max} by using Eqs. 2-4, as follows. First, E_2 was calculated from P_O^{max} (Eq. 4). Second, K_{dC} was calculated from E_2 and EC_{50} (Eq. 3). Third, K_{dO} was calculated from E_2 and K_{dC} using a known value of E_o (Eq. 2). Finally, efficiency was calculated from the two equilibrium dissociation constants (see Materials and Methods and ref 5),

$$\eta=1-\log K_{dC}/\log K_{dO} \qquad \text{Eq. 5}$$

Four previous results enabled us to estimate efficiency from a CRC. First, adult AChR binding sites have approximately the same affinity, so only single values of the 2 equilibrium dissociation constants needed to be estimated for each ligand. Second, Scheme 1 has been proved experimentally, so K_{dC} could be calculated using Eqs. 3 and 4. Third, the unliganded gating equilibrium constant E_o is known so K_{dO} could be calculated by using Eq. 2. In an 'efficiency" plot for a group of ligands (5), E_o is estimated from the y-intercept. However, prior knowledge of E_o is required to estimate efficiency from a single CRC.

ACh efficiency

Plots of P_O versus [agonist] were constructed from single-channel currents (Fig. 2). The leftmost trace in Fig. 3A shows a previously-published CRC for ACh in adult-type mouse AChRs (8). We fit these P_O values by Eq. 1 with the result P_O^{max}=0.96 and EC_{50}=43 μM (Table 1). From P_O^{max} we calculate that the diliganded gating equilibrium constant is E_2=23.4 (Eq. 4). From this value and EC_{50} we calculate that the low-affinity equilibrium dissociation constant is K_{dC}=174 μM (Eq. 3). The unliganded gating equilibrium constant at +70 mV is $E_o=5.2\times10^{-7}$ (see Materials and Methods) so we calculate that the high-

1 affinity equilibrium dissociation constant is K_{dO}=26 nM (Eq. 2). Finally, from the ratio of

2 the logs of the two equilibrium dissociation constants we calculate η_{ACh}=50% (Eq. 5).

Fig. 2

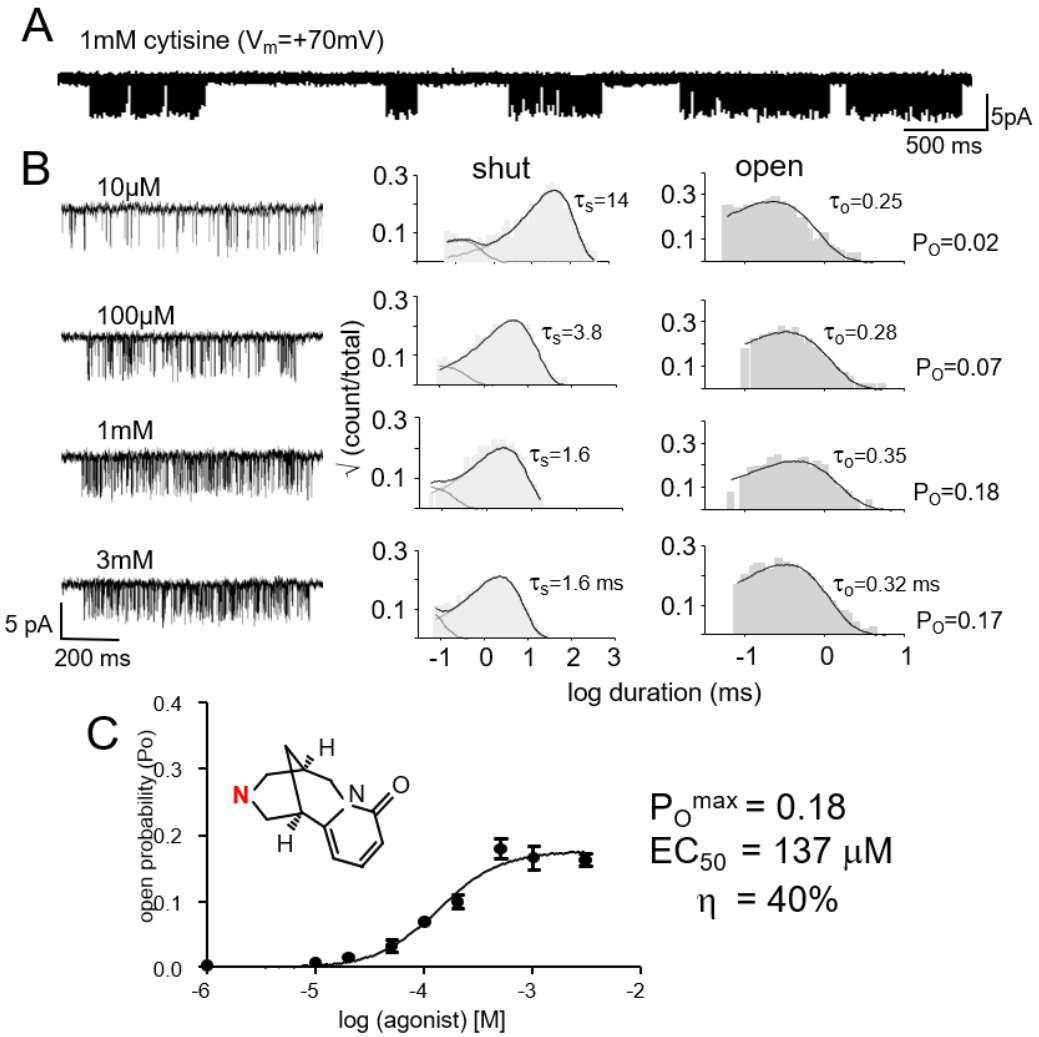

Figure 2. Activation of adult-type AChRs by cytisine. A. Low-resolution view of single-channel currents showing clusters of openings arising from a single AChR, separated by silent periods when all AChRs in the patch are desensitized (V_m, membrane potential). B. High-resolution views of example clusters at different [agonist] and corresponding interval-duration histograms. The predominant intra-cluster shut and open interval durations (τ_s and τ_o) were used to calculate an open-channel probability (P_O) at each agonist concentration. C. CRCs fitted by Eq. 1 to estimate EC_{50} and P_O^{max} (symbols, mean±s.e.m.). Efficiency (η) was calculated from the CRC parameters by using Eqs. 2-5.

Fig. 3

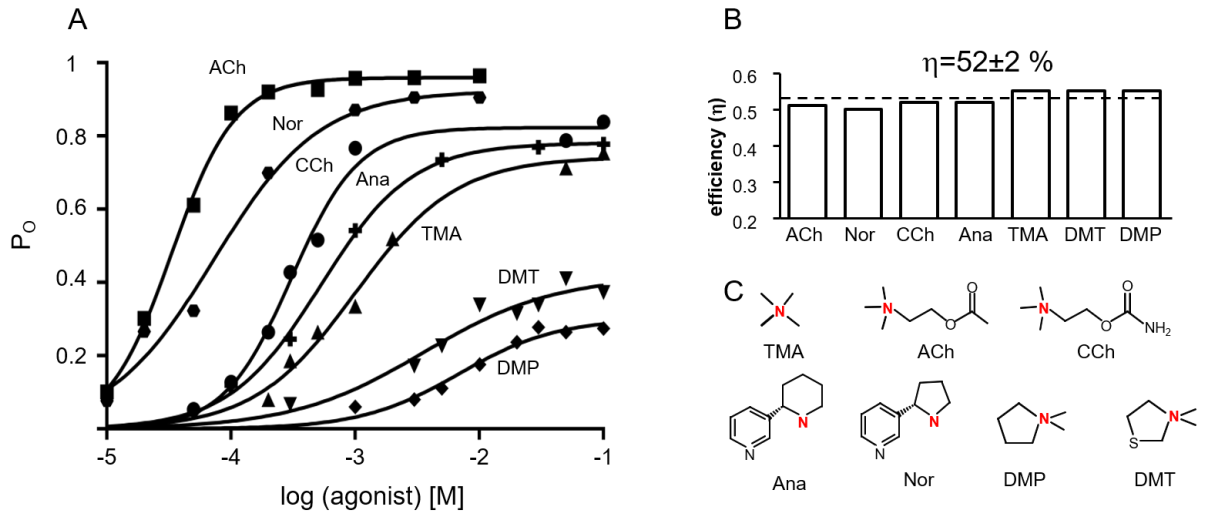

Figure 3. Estimates of agonist efficiency from previously-published CRCs. A. CRCs of 7 agonists on adult-type mouse AChRs from (8). For these ligands there is an inverse correlation between EC_{50} and P_O^{max} (Table 1). B. Agonist efficiencies calculated from EC_{50} and P_O^{max}. All agonists have approximately the same efficiency of 52 ± 2 % (mean±s.d., dashed line). C. Agonist structures. Tetramethylammonium (TMA), acetylcholine (ACh), carbamylcholine (CCh), anabasine (Ana), nornicotine (Nor), dimethylpyrrolidium (DMP) and dimethylthiazolidinium (DMT). Red, key nitrogen atom in the agonist's head group.

Macroscopic CRCs for ACh and adult-type, human AChRs have been measured using automated patch clamp and whole cell currents, with the result EC_{50}=22 μM (9). A macroscopic current amplitude is equal to the product of the number of receptors contributing to the response, the single-channel current amplitude and P_O. Because the number of receptors is unknown in these experiments, an absolute P_O^{max} (that pertains to Scheme 1) could not be estimated. However, using our single-channel value P_O^{max}(ACh)=0.96 and E_o=4.5x10^{-7} (V_m=-60 mV), we calculate from the whole-cell CRC that η_{ACh}=49% (Table 1).

In addition, we calculated η_{ACh} from published values of K_{dC} and K_{dO} either from wild-type mouse AChRs (8) or from individual α–δ and α–ε human AChR binding sites (2), in both instances estimated by kinetic modeling of single-channel currents. The efficiencies calculated from these independent datasets are both 50% (Table 1).

These results indicate that at adult AChR binding sites about half of the available neurotransmitter binding energy is applied to the gating conformational change. That is, the energy of ACh binding to C is approximately half that of binding to O, and (for 2 sites) is about equal to the energy of diliganded gating. Further, the results show that agonist efficiency in AChRs can be estimated from single-channel or whole-cell CRCs (as long as contamination by desensitization is avoided by using fast agonist application), is the same whether receptors have one or two functional neurotransmitter binding sites, and is similar in mouse and human adult-type AChRs.

Efficiency of other agonists

1 We fitted other previously published CRCs to estimate EC_{50}, P_O^{max} and η (Fig. 3A;
2 Table 1). Despite the wide ranges in both EC_{50} (43 μM to 6.7 mM) and P_O^{max} (0.26 to
3 0.96), all 7 of these agonists (including ACh) have approximately the same efficiency,
4 η=52±2% (mean±s.d) (Fig. 3B).

Fig. 4

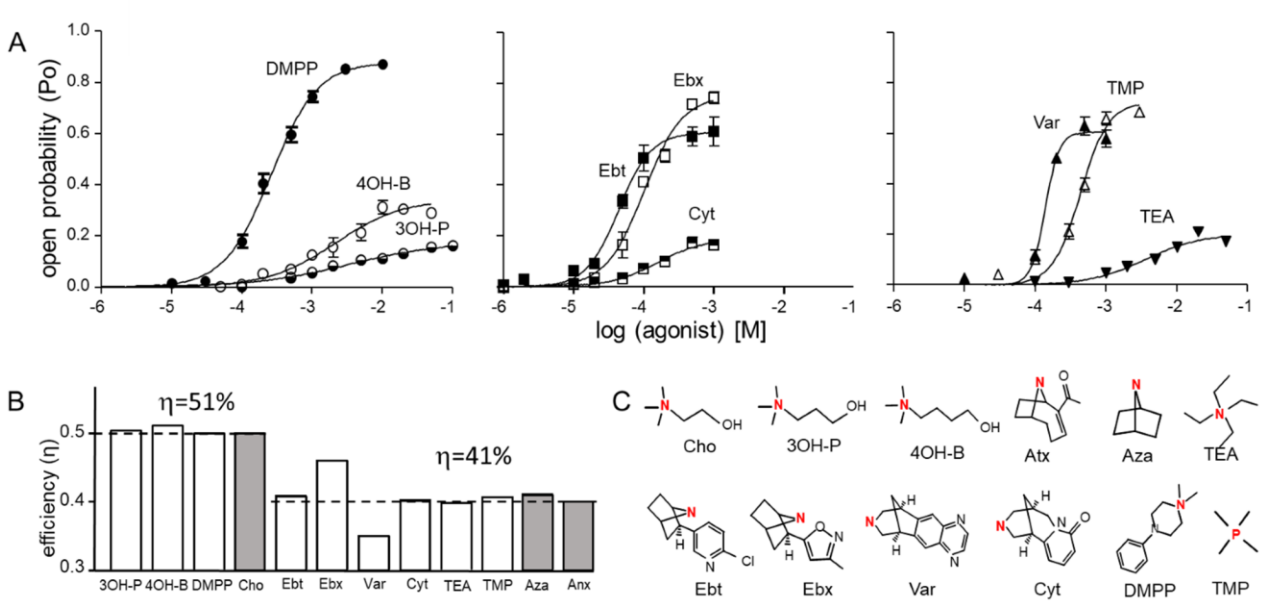

Figure 4. Estimates of agonist efficiency from newly-measured CRCs. A. CRCs (symbols, mean±s.e.m.). Background mutations were used to eliminate channel block (εS450W; left and middle) or to increase P_O^{max} and left-shift EC_{50} by increasing the constitutive gating equilibrium constant (εL269F+εE181W; right). EC_{50} and P_O^{max} values in Table 1 have been corrected for these backgrounds and pertain to adult, wild-type mouse AChRs. Interval-duration histograms with corresponding predominant intra-cluster shut and open interval durations and example clusters can be found in SI (figure 4 – figure supplement 1-3). B. Efficiencies calculated from the CRCs (open bars) or from previously-reported measurements of K_{dC} and K_{dO} obtained by kinetic modeling (2) (gray bars). There are 2 populations with average efficiencies of 51 % and 41% (dashed lines). C. Agonist structures. Choline (Cho), 3-hydroxypropyltrimethylammonium (3OH-PTMA), 4-hydroxybutyltrimethylammonium (4OH-BTMA), anatoxin (Atx), azabicycloheptane (Aza), tetraethylammonium (TEA), epibatidine (Ebt), epiboxidine (Ebx), varenicline (Var), cytisine (Cyt), dimethylphenylpiperazinium (DMPP), tetramethylphosphonium (TMP). Key nitrogen or phosphorous atom in the head group is shown in red.

Table 1

		Measured Values			Calculated values						
	agonist	**EC_{50} (μM)**	**P_O^{max}**	**n**	**E_2**	**K_{dC} (μM)**	**λ**	**K_{dO} (nM)**	**log K_{dC}**	**log K_{dO}**	**η**
1	ACh[ł]	43	0.96	-	23.4	174	7210	24	-3.76	-7.62	***0.50***
	ACh[Φ]					130		18	-3.89	-7.74	***0.50***
	ACh[Ψ]	22	0.96		24	90	7303	12	-4.04	-7.91	***0.49***
2	Nor[±]	72	0.92	-	12	200	5161	38	-3.70	-7.41	***0.50***
3	CCh[ł]	320	0.84	-	5.25	542	3416	159	-3.27	-6.80	***0.52***
4	Ana[±]	524	0.78	-	3.63	719	2840	253	-3.14	-6.60	***0.52***
5	TMA[ł]	1200	0.75	-	3	1480	2582	574	-2.83	-6.24	***0.54***
6	DMT[ł]	4200	0.42	-	0.72	2730	1269	2150	-2.56	-5.67	***0.54***
7	DMP[ł]	6700	0.26	-	0.35	3570	884	4040	-2.45	-5.39	***0.54***
8	Cho*	4013	0.05	-	0.05	4100	297	15100	-2.39	-4.82	***0.50***
9	DMPP[1]	246±81	0.87±0.09	3	6.69	480	3587	134	-3.32	-6.87	***0.52***
10	4OH-B[1]	2171±77	0.29±0.04	3	0.41	1270	886	1350	-2.92	-5.87	***0.50***
11	3OH-P[1]	3485±10	0.15±0.02	4	0.18	1660	583	2840	-2.78	-5.55	***0.50***
12	Ebt[1]	32±2	0.60±0.6	4	1.50	28	1698	16	-4.55	-7.78	***0.41***
13	Ebx[1]	90±4	0.74±0.02	3	2.85	108	2340	46	-3.96	-7.33	***0.46***
14	Cyt[1]	137±5	0.18±0.01	4	0.22	67	650	104	-4.17	-6.99	***0.40***
15	Var[2]	135±12	0.015±0.002	3	0.02	57	171	331	-4.25	-6.48	***0.35***
16	TEA[2]	4200±130	0.002±0.0007	3	0.002	174	65	26800	-2.76	-4.57	***0.40***
17	TMP[2]	844±32	0.03±0.002	3	0.031	360	244	1473	-3.44	-5.83	***0.41***
18	Atx[‡]					115		247	-3.94	-6.61	***0.40***
19	Aza[‡]					934		6053	-3.03	-5.22	***0.42***

Table1. EC_{50} and P_O^{max} were obtained by fitting each CRC to Eq. 1 (for multiple P_O measurements as mean± s.e.m.). Calculated equilibrium constants diliganded gating (E_2) and dissociation to C or O (K_{dC} or K_{dO}); coupling constant λ=sqrt(E_2/E_0) (Eq. 2); η=efficiency (Eq. 5). Previously-published values from [ł] (8), [±] (10), [Φ] (2), [Ψ] (9), * (11), [‡] (5). Values after correction for background mutations that increase E_0, [1]εS450W and [2](εL269F+εE181W).

Next, we measured efficiencies for other agonists that were not studied previously by CRCs (Fig. 4). Choline (Cho) has 2 methylenes between its quaternary nitrogen and hydroxyl (OH) group versus 3 and 4 for 3OH-BTMA and 4OH-PTMA. Cho is a low-affinity, low-efficacy agonist (11) that K_{dC} and K_{dO} values estimated by modeling single-channel kinetics of the human α–ε site indicate has the same efficiency as ACh, η_{Cho}=52% (5). Simulations of binding site structures suggest that an H-bond between the terminal OH and the backbone carbonyl of αW149 serves to position the charged nitrogen of choline away from the aromatic rings that line the cavity, to reduce favorable binding energy (12, 13). Inserting additional methylenes reduces the probability of this H-bond and allows a more-optimal position that increases binding energy relative to Cho.

The CRCs and associated P_O^{max} and EC_{50} values for 3OH-BTMA and 4OH-PTMA are shown in Fig. 4A left. From the calculated equilibrium dissociation constants we estimate η=50% for both of these agonists (Table 1). Despite the substantial range in affinity and efficacy afforded by the different H-bond propensities, all three of the choline-based agonists have the same efficiency that is the same as for the agonists shown in Fig. 3. The similarity in the C versus O binding energy *ratio* (but not the difference) for these 3 ligands suggests that the effect of the H-bond on the position of the nitrogen atom applies equally to C and O binding cavities.

Fig. 4A left also shows the CRC of dimethylphenylpiperazinium (DMPP), a nicotinic receptor agonist that is selective for the α3β4 (ganglionic) subtype (14). The result was η_{DMPP}=52%.

Overall, the mean±s.d efficiency calculated from CRCs for the 11 agonists described so far (ACh, Nor, CCh, Ana, TMA, DMP, DMT, Cho, 4OH-BTMA, 4OH-PTMA, DMPP) is

52±2 %. For this group of ligands, the binding energy ratio $\log K_{dC}/\log K_{dO}$ is 0.48, indicating that on average the agonist binding energy increases by a factor of ~2.1 when the sites switch spontaneously from C to O.

Fig. 4A middle shows CRCs for 3 agonists that have a bridge nitrogen atom. The efficiency values for epibatidine, epiboxidine and cytisine calculated from P_O^{max} and EC_{50} were η_{Ebt}=41%, η_{Ebx}=46% and η_{Cyt}=40%. The first two values are similar to those estimated previously by kinetic modeling at the human α–δ binding site (5).

Fig. 4A right shows CRCs for agonists that have an extraordinarily low efficacy and affinity. To study these we added background mutations that did nothing more than increase E_0 and, hence, increase P_O^{max} and left-shift EC_{50} (Eqs. 2-4). After correcting for the effects of the background mutations, from the CRC parameters we estimate that η_{TEA}=40%, η_{TMP}=41% and η_{var}=35%.

For the group of 6 ligands shown in Fig. 4A middle and right (Ebt, Ebx, Cyt, Var, TEA, TMP) the average efficiency 41±4% (Fig. 4B). For these ligands, the binding energy ratio ($\log K_{dC}/\log K_{dO}$) is 0.60, indicating that binding energy increases by a factor of ~1.7 when the sites switch spontaneously from C to O.

Fig. 5A shows a histogram of efficiency values for 17 agonists estimated from CRCs plus 2 agonists estimated from single channel kinetic modeling (Atx, Aza; Fig. 4C) (5). A goodness of fit test indicates that a bimodal (sum of two Gaussians) frequency distribution is a better fit than a single Gaussian ($F(3,16) = 3.37$, $P=0.044$). The two populations have efficiencies of 51±0.02% and 40±0.01% (mean±s.d.), which are comparable to mean efficiencies of the two agonist-groups discussed above.

Fig. 5

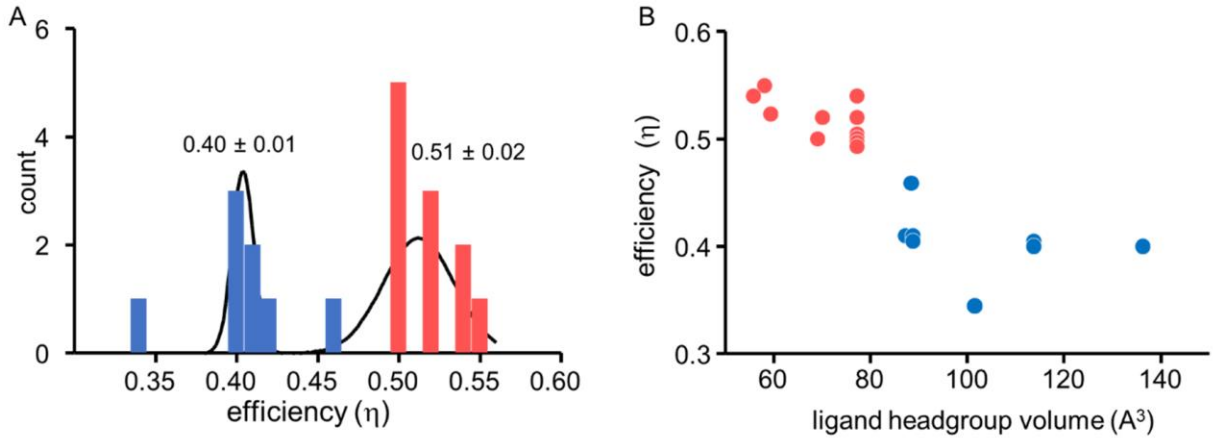

Figure 5. Distribution of agonist efficiency. A. Efficiencies for 19 agonists (17 from CRCs, 2 from kinetic modeling). Bi-modal distribution of efficiencies fitted by the sum of two Gaussians. There are 2 efficiency populations, η=51 ± 0.02 % and 40 ± 0.01 % (mean±s.d.). B. 2-D scatter plot of efficiency versus head-group volume (v). Cluster analysis (k-means) shows 2 populations with centroids (η/v) of 52%/70.4 A^3 and 41%/102.2 A^3.

We also estimated the volumes of the 'head' group of the agonists (v) and plotted these versus efficiency (Fig. 5B). A 2D cluster analysis again shows 2 populations with efficiencies of η_1=52% (n=11) and η_2=41% (n=8) with corresponding volumes of v_1=70.4±8.8 and v_2=102.2±17.8 Å^3 (centroid±s.d.) respectively. There is an inverse relationship between agonist efficiency and head-group volume.

Binding site mutations. K_{dC} and K_{dO} have been estimated by kinetic modeling of single-channel currents from mouse, adult-type AChRs having a mutation of an aromatic residue at both binding sites (15). We calculated from these values η_{ACh} for 22 different mutants. Figure 6 shows Gaussian distribution with η_{ACh}=51±4% (centroid±s.d.), which is the same as in wt AChRs (Fig. 1). The one clear exception was αY190A that falls outside the distribution, for which η^{ACh} =35%. The three largest efficiency-values were for mutations of αW149 (Figure 6–Source Data 1 in SI).

Utility of efficiency. Knowledge of η simplifies and extends CRC analysis. The same efficiency for a group of agonists means the same $\log K_{dC}/\log K_{dO}$ ratio and, hence, that the two dissociation constants are related by the same exponent, $K_{dC}=K_{dO}^{0.48}$ for the higher efficiency population and $K_{dC}=K_{dO}^{0.60}$ for the lower efficiency population. Hence, given this exponent (equal to 1-η), one equilibrium dissociation constant can be calculated from the other. This has two useful consequences.

First, knowledge of η (along with the agonist-independent constant E_o) allows the estimation of EC_{50} from P_O^{max} that is the response at a single, high [agonist]. Combining Eqs. 2 and 5 and rearranging yields

$$\log E_2 = [2\eta/(\eta-1)]\log K_{dC} + \log E_0. \qquad \text{Eq. 6}$$

E_2 can be calculated directly from P_O^{max} (Eq. 4), so with knowledge of η one can solve Eq. 6 for K_{dC}, then Eq. 3 for EC_{50}.

Fig. 6

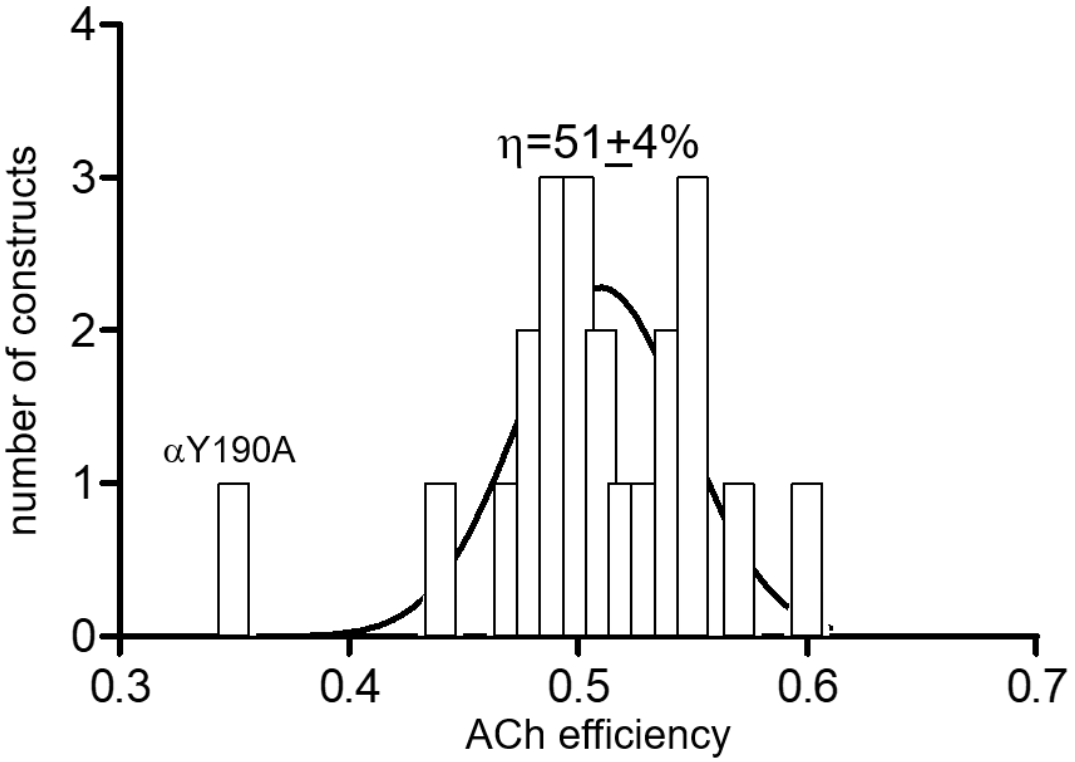

Figure 6. ACh efficiency in AChRs having binding site mutations. Mutations were at both adult-type binding sites (15): αY93 (W,H,A,F, S), αW149 (F, Y, A), αY190 (F, W, A), αY198 (F,H,W,S,T,L,A), εP121 (L,Y,G). The only mutation that altered ACh efficiency significantly was αY190A, reducing it from the higher- to the lower-efficiency population (from 50% to 35%). αY190F and αY190W did not alter ACh efficiency. Gaussian fit of frequency distribution was η=51±4 % (mean±s.d). Refer Figure 6–Source Data 1 in SI for individual ACh efficiencies of mutant receptors.

Fig. 7

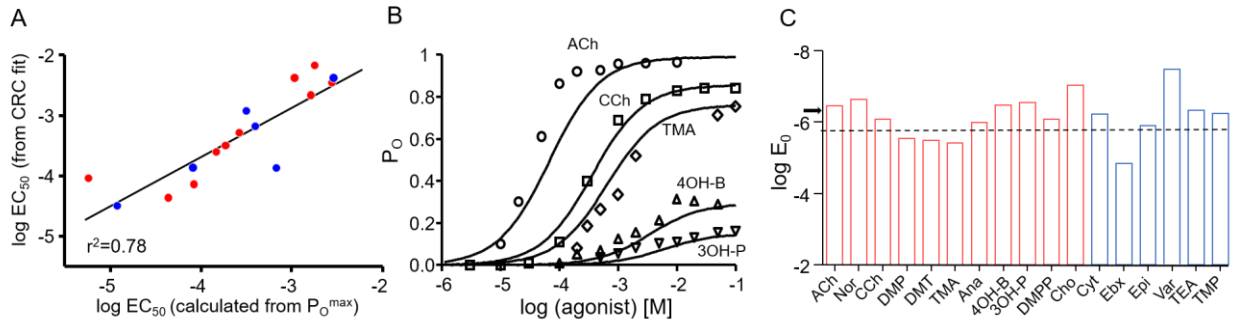

Figure 7. Using efficiency to estimate affinity from efficacy, and unliganded gating. A. If an agonist's efficiency and the receptor's E_0 are known, EC_{50} can be calculated from P_O^{max}. Log-log plot of EC_{50} values obtained by calculation versus by fitting CRCs. Linear fit slope=0.83, r^2=0.78; red, η=52% and blue, η=41% (Fig. 4). Refer Figure 7–Source Data 1 in SI for EC_{50} values calculated from P_o^{max} in plot 7A. B. P_o values at different [agonist] calculated from only P_O^{max} values (lines) agree with experimental P_O measurements (symbols). Solid lines calculated using $P_o=x^2.E_2/(1+2x+x^2+x^2E_2)$ where $x=[A]/K_{dC}$ (7). C. If an agonist's efficiency is known, the unliganded gating equilibrium constant (E_0) can be calculated from constants derived from EC_{50} and P_O^{max} (Eq. 6). The assumed η values were either 52% (red) or 41% (blue). The calculated mean E_0 of 1.1 x 10^{-6} (dashed line) is approximately the same regardless of η and reasonably close to the E_0 value estimated using other methods (arrow). So-calculated E_0 for 17 agonists are given in Figure 7–Source Data 2 (SI).

Figure 7A shows EC_{50} values so-calculated assuming η is either 52% or 41% (Fig. 5B). The calculated EC_{50} values match those obtained by fitting experimental CRCs (Pearson's correlation, r^2=0.78, P<0.0001). Further, Fig. 7B shows that only high-concentration asymptote can be used to calculate responses at all agonist concentrations. If agonist efficiency and the unliganded gating constant are known, an entire CRC can be estimated from the response at just one [agonist].

Diliganded gating equilibrium constants, from which P_O^{max} can be calculated (Eq. 4), have been measured experimentally for many AChR agonists (13). Table 2 shows the predicted EC_{50} values calculated using Eq. 6 assuming that η=52%.

Second, knowledge of η allows the estimation of the unliganded gating equilibrium constant (E_o) from a single CRC. E_o is an important, ligand-independent constant that sets the basal level of activity (the low-concentration asymptote of the CRC, usually mistaken to be zero) from which agonists increase P_O, but it is often quite small and difficult to measure directly (16-18). The procedure to estimate E_o from a CRC of a wt receptor is first to solve for E_2 and K_{dC} from P_O^{max} and EC_{50} as described above, then solve for E_o using Eq. 6. Fig. 7C shows E_o values so-calculated from CRC parameters using assumed η-values of 52% or 41%. The mean result for V_m=-100 mV, 1.1±2 x 10^{-6} (mean±s.d), is reasonably close to the experimentally-determined value of 7.4 x 10^{-7} (19). If agonist efficiency is known, an approximate value of the unliganded gating constant can be estimated from a single CRC. Once this value has been learned, it can be applied to all agonists.

Table 2

Input values				Calculated values					
Ligand	**E_2**	**η**	**E_0**	**P_{omax}**	**log E_0**	**log E_2**	**log E_2-logE_0**	**K_{dC} (mM)**	**EC_{50} (mM)**
TMA	2.54	0.52	5.2E-7	0.72	-6.28	0.40	6.69	0.82	0.49
ETMA	0.25	0.52	5.2E-7	0.20	-6.28	-0.60	5.68	2.39	2.86
PTMA	0.29	0.52	5.2E-7	0.22	-6.28	-0.54	5.75	2.61	2.61
BTMA	2.44	0.52	5.2E-7	0.71	-6.28	0.39	6.67	0.83	0.51
Cho	0.05	0.52	5.2E-7	0.05	-6.28	-1.30	4.98	5.01	6.84
3OH-P	0.15	0.52	5.2E-7	0.13	-6.28	-0.82	5.46	3.02	3.85
4OH-B	0.71	0.52	5.2E-7	0.42	-6.28	-0.15	6.14	1.47	1.42
Cl Cho	0.19	0.52	5.2E-7	0.16	-6.28	-0.72	5.56	2.71	3.37
2OH-P	0.02	0.52	5.2E-7	0.02	-6.28	-1.70	4.59	7.65	10.7
Cholamine (pH 9.0)	0.04	0.52	5.2E-7	0.04	-6.28	-1.40	4.89	5.56	7.63

Table 2: EC_{50} values calculated (Eq. 6) from published diliganded gating equilibrium constants (E_2) (20). TMA (tetramethyl ammonium), ETMA (ethyltrimethyl ammonium), PTMA (propyltrimethyl ammonium), BTMA (butyltrimethyl ammonium), Cho (Choline), 3OH-PTMA (3-hydroxypropyl trimethyl ammonium), 4OH-BTMA (4-hydroxybutyl trimethyl ammonium), Cl Cho (2-chloroethyl trimethyl ammonium), 2OH-PTMA (2-hydroxypropyl trimethyl ammonium), cholamine (2-aminoethyl trimethyl ammonium)

Discussion

The main results are that in adult-type AChRs, agonist efficiency i) can be estimated from a CRC, ii) is ~50% for the neurotransmitter ACh and its breakdown product choline, iii) has a bi-modal distribution, iv) is correlated inversely with head-group volume, and v) simplifies and extends CRC analysis. Further experiments are needed to explore the structural basis of agonist efficiency in AChRs, and whether or not groups of structurally-related agonists have a common efficiency in other receptors.

Estimating efficiency. The estimates of agonist efficiency are the same whether obtained from single-channel or whole-cell currents, from a CRC or by detailed kinetic modeling. They are the same in wt AChRs with 2 active binding sites or in AChRs that have just 1 active site. Efficiency is approximately the same in mouse and human AChRs, and in receptors that have a mutation of a binding site aromatic residue (except for αY190A) or in distant regions that do not affect affinity. In AChRs, efficiency is a robust agonist attribute. At neuromuscular synapses, about half of the available neurotransmitter binding energy is converted into mechanical energy for the gating conformational change.

Many agonists have the same efficiency as ACh. An efficiency of ~50% implies that for these ligands the binding energy to O is approximately double that to C, regardless of affinity and efficacy (8). Further, a constant efficiency implies that the energy change in low-affinity *binding* to C ($\log K_{dC}$) is a constant fraction of (for ACh, about equal to) the energy change of the switch from low-to-high affinity ($\log K_{dO}$-$\log K_{dC}$) that happens inside C-to-O *gating* (5, 8). That is, binding and gating energies are correlated.

Low-affinity binding to C is slower than diffusion (8) and is associated with a structural rearrangement of the binding site called 'catch'. The structural change at the

binding site associated with the low-to-high affinity switch in conformation (that takes place within gating) is called 'hold'. [Note: 'hold', 'flip' (21) and 'prime' (22) all refer to intermediate events within the gating transition. See (23) for a discussion.] A constant efficiency for a group of agonists implies that there is a linear correlation between binding (catch) and gating (hold) energies that in turn suggests these two rearrangements of the binding site are related. The correlation between catch-and-hold energies and, possibly, structural changes blurs the distinction between binding and gating. In AChRs, the forward allosteric transition begins with ligand association, with binding-gating (catch-and-hold) appearing as two stages of a single, amalgamated structural (energy) change process.

It remains to be determined whether or not a constant efficiency for a group of related agonists is particular to neuromuscular nicotinic AChRs or is a general feature of receptor activation. It appears that in some other receptors there is a linear relationship between log gating and log binding equilibrium constants for structurally-related ligands, suggesting that for these there is a constant $\log K_{dC}/\log K_{dO}$ ratio and, hence, a constant efficiency (5), but more experiments are needed.

Bimodal distribution. There are 2 populations of AChR agonist efficiency values, at 52±2% and 41±4%. The small s.d. for each population suggests that most of the variation likely arises from measurement error rather than from actual, ligand-specific differences. Further evidence of bi-modality in efficiency comes from the observation that the binding site mutation αY190A shifts the efficiency of ACh from 51% to 35%, or from the high-efficiency group into the low-efficiency group (same as varenicline). The results so far suggest that the distribution of agonist efficiency is modal rather than continuous, but

more ligands need to be examined to determine if other efficiencies are possible. It is also possible that more extensive and precise measurements might reveal consistent efficiency differences consequent to binding site mutations. For example, the the observation that Y, F and A substitutions at αW149 have slightly higher ACh efficiencies compared to the wt needs to be investigated by examining more mutations and agonists.

Structural correlates. Changes in protein structure, dynamics or both undergird the conversion of chemical binding energy into mechanical gating energy. Although our experiments did not address directly the important question of understanding the molecular events that determine that 50% versus 40% of the agonist's binding energy is applied to the gating conformational change, there are some clues.

Members of both efficiency groups (high, low) may have a quaternary amine (TMA, TEA) or a secondary amine (DMPP, Ebt). Hence, it does not appear that the bimodal distribution in efficiency reflects differences in the charge on the agonist's head group nitrogen (or phosphorous, in the case of TMP).

The inverse correlation between agonist head-group volume and efficiency may be more relevant (Fig. 5B). Simulations of AChR structures suggest the possibility that the agonist binding cavity is smaller in O compared to in C (12). Further, kinetic analyses of AChR gating suggest that channel-opening occurs as a sequence of domain motions with the energy change of the extracellular domain (a contraction or 'unblooming'; (24)) following the 'hold' energy change at the binding cavity (25). Hence, it is possible that larger-volume, lower-efficiency agonists encounter steric hindrance when the cavity shrinks, to limit the extent of the contraction and, hence, the force applied to the next region of the protein to move in the gating sequence, the extracellular domain. We

hypothesize that the higher-efficiency ligands fit comfortably into both the C and O pockets but lower-efficiency agonists do not fit easily into O. Accordingly, pocket contraction is more-limited with lower-efficiency agonists, so less energy for gating is generated by the binding site's 'hold' rearrangement. However, the relationship between volume and efficiency is not simple because Ebt and TEA have similar efficiencies despite there being a substantial difference in head-group volume.

That there are 2 discrete efficiency populations suggests there could be two discrete pathways that couple binding energy to gating, for instance one that supplies ~40% of the energy and another than supplies ~10%. Perhaps with smaller agonists both pathways are utilized, but when the binding pocket is 'stretched' by a large agonist either the 10% pathway is broken, or both are compromised.

Another clue regarding the structural basis of efficiency is that the only binding site mutations that changed significantly the efficiency of ACh was αY190A, reducing it from the high to the low population. This suggests that perturbation of αY190 is part of a pathway for some (10%?) of the energy that is transferred out of the binding pocket (20, 26). However, the fact that the mutations αY190F and αY190W have no effect on ACh efficiency suggests that the key interaction is with the aromatic ring rather than with the OH group. Measuring the effects of mutations on agonist efficiency may be an effective way to explore molecular pathways by which energy is transferred from the binding site into the extracellular domain, and beyond.

The efficiency estimates for the two populations are the same whether measured in whole receptors (that have α–δ and α–ε binding sites) or in receptors having only one

functional site (5). This indicates that the energy changes that contribute to efficiency are determined mainly by local ligand-protein interactions at each binding site, with little or no energy transfer between sites. The efficiency of Ebx is somewhat higher in whole receptors compared to at α–δ alone so it is possible that the efficiency of this agonist is modestly greater at one site (α–ε) compared to the other.

Utility of efficiency. Knowing agonist efficiency is useful because it allows EC_{50} from P_O^{max} (affinity to be estimated from efficacy). That is, an entire CRC can be estimated from an experimental measurement at just one agonist concentration. This ability could greatly facilitate drug screening. The above results raise the possibility that it may someday be possible to predict agonist efficiency *a priori* from ligand and binding site structures (head-group and binding-cavity volumes), in which case the need for wet-bench experiments in CRC estimation would be reduced substantially.

There are stipulations with regard to calculating agonist efficiency from a CRC. First, the CRC must be comprised of absolute responses rather than normalized to the maximum. Normalized CRCs are more common because it is difficult to know the number of receptors contributing to the response. Our approach (single-channels) circumvents this problem by ensuring that exactly 1 receptor contributes to each P_O measurement. One way to make a CRC from absolute, whole-cell responses is to count the number of receptors (27) or to calibrate each response to that of an agonist having a known, absolute response. Second, the CRC should be largely uncontaminated by events outside the core activation scheme (Fig. 1). Whole-cell responses arising from multiple receptor populations (heterogeneity) or generated by slow agonist application (desensitization) may not produce CRCs that match Eqs. 3 and 4. For some receptors the equations that

relate CRC parameters with binding and gating constants may be more complicated. The extent to which such contaminations influence the efficiency estimate from a whole cell CRC remains to be determined and could be different for different receptors. Third, E_0 must be known *a priori*. However, this constant applies to all agonists and only needs to be measured once for each receptor.

Materials and Methods

Experimental design

Expression. Human embryonic kidney (HEK) 293 cells were maintained in Dulbecco's minimal essential medium supplemented with 10% fetal bovine serum and 1% penicillin–streptomycin, pH 7.4. AChRs were expressed by transient transfection of mouse α, β, δ and ε subunits in the ratio 2:1:1:1 (*Trans*IT® 293 transfection reagent; Mirus Bio, Madison, WI). Electrophysiological experiments started ~48 hours post-transfection. No animals were used in this study.

Electrophysiology. Single-channel currents were recorded in the cell-attached patch configuration at 23° C. The bath solution was (in mM): 142 KCl, 5.4 NaCl, 1.8 $CaCl_2$, 1.7 $MgCl_2$, 10 HEPES/KOH (pH 7.4). Patch pipettes were fabricated from borosilicate glass and fire polished to a resistance of ~10 MΩ when filled with the pipette solution that was Dulbecco's phosphate-buffered saline (in mM): 137 NaCl, 0.9 $CaCl_2$, 2.7 KCl, 1.5 KH_2PO_4, 0.5 $MgCl_2$, and 8.1 Na_2HPO_4 (pH 7.3/NaOH). Currents were recorded using a PC505 amplifier (Warner instruments, Hamden, CT), low-pass filtered at 20 kHz and digitized at a sampling frequency of 50 kHz using a data acquisition board (SCB-68, National instruments, Austin, TX). Agonists were added to the pipette solution at the desired concentration.

Analysis. Fig. 1 shows the main states involved in AChR activation and de-activation. When the agonist association and opening rates are sufficiently large, single-channel openings occur in clusters (28) (Fig. 2). Shut intervals within clusters represent mainly agonist binding and receptor gating (Fig. 1, bold) whereas shut intervals between clusters

represent mainly long-lived desensitization (not shown in Fig. 1). We selected for analysis clusters that appeared by eye to arise from a homogeneous open probability (P_O) population and limited the analysis to intra-cluster interval durations.

Because of the high extracellular [K^+], the cell membrane potential (V_m) was 0 mV. The AChR agonists we examined also are channel-blockers. To both generate measurable outward currents and reduce the effect of channel block on P_O, the membrane was depolarized to +70 mV by holding the pipette at -70 mV. This effectively eliminated agonist binding to the channel-block site in the transmembrane domain but did not affect agonist binding to the neurotransmitter sites in the extracellular domain.

Analyses of the currents were performed by using QUB software (29). A cluster was defined as a group of openings flanked by shut intervals longer than some duration that depended on the [agonist] (t_{crit}, range 7-20 ms). Open and shut currents within clusters were idealized into noise-free intervals by using the segmental k-means algorithm (SKM) after digitally low-pass filtering the data at 10 kHz (30).

The idealized interval durations were fitted by multiple exponential components using a maximum interval likelihood algorithm (MIL) (31). Cluster P_O at each [agonist] was calculated from the time constants of the predominant components of the shut-time (τ_s) and open-time distributions (τ_o): $\tau_o/(\tau_s+\tau_o)$ (Fig. 2, Figure 4 – figure supplement 1-3). The half-maximum (EC_{50}) and maximum (P_o^{max}) response were estimated by fitting to an empirical equation (Eq.1) using GraphPad Prism 6.

Definitions.

The agonist binding free energy is equal to +RTln(K_{dC}) or +RTln(K_{dO}), where R is the gas constant and T is the absolute temperature. In our experiments, RT=0.59. Agonist

efficacy (P_O^{max}) depends only on the gating equilibrium constant (Eq. 4) that in turn depends on the K_{dC}/K_{dO} ratio (Eq. 2) or, in terms of energy, $\log(K_{dC})-\log(K_{dO})$. That is, agonist efficacy is a function of the *difference* between C and O binding energies. Partial agonists experience smaller increases in O versus C binding energy compared to full agonists, antagonists experience no change in binding energy, and inverse agonists experience a decrease in favorable binding energy upon receptor activation.

In contrast, agonist efficiency depends on the *ratio* of binding energies, as shown previously (5) and as follows. Agonist activation of a resting, unliganded AChR entails connecting the resting-unliganded state C to the diliganded-active state A_2O (Fig. 1). Because microscopic reversibility is satisfied (2), the product of the equilibrium constants (sums of the energy changes) for the steps linking these states in the clockwise direction (the main physiological activation route) is the same as in the counter-clockwise direction. The product of the counter-clockwise equilibrium constants is E_o/K_{dO}^2, the negative log of which gives the *total* energy required for activation by this route, $2\log(K_{dO})-\log E_o$. The product of the equilibrium dissociation constants connecting C with A_2C is $1/K_{dC}^2$, the negative log of which is the energy for just the *binding* part of activation by the clockwise route, $2\log(K_{dC})$. We are interested only in the agonist component of the total energy and, because $\log E_o$ is the same for all agonists it can be ignored (set to 0). We now calculate agonist efficiency from these energies. The fraction of the total energy that is used in binding is $2\log K_{dC}/2\log K_{dO}$, and the efficiency, which the fraction that pf the total applied to gating, is $1-\log K_{dC}/\log K_{dO}$ (Eq. 5).

<u>*Voltage, E_o and background mutations*</u>. Depolarization to V_m=+70 mV (to reduce channel block by the agonist) has the undesired consequence of shortening τ_o making

current detection and idealization more difficult. To compensate, we added the background mutation εS450W (in the M4 transmembrane segment of the ε subunit) that has the equal-but-opposite effect on gating as does depolarization by +140 mV, but has no effect on agonist binding (32). With this mutation, τ_o and the unliganded gating equilibrium constant E_o at +70 mV were the same as in wild-, adult-type AChRs at V_m=-70 mV. E_o at -100 mV is 7.4 x 10^{-7} and is reduced e-fold by a 60 mV depolarization (19). Hence, we estimate that in our experiments at V_m=+70 mV and with εS450W, E_o is 5.2 x 10^{-7}.

With the low-efficacy agonists varenicline, tetraethylammonium and tetramethylphosphonium currents clusters generated by wild-type (wt) AChRs were poorly defined because the channel-opening rate constant was too small. For these ligands P_O could not be estimated accurately using wt AChRs. To increase the diliganded opening rate constant and generate better-defined, higher-P_O clusters we added two background mutations in the ε subunit, εL269F (in the M2 helix) and εE181W (in strand β9), without εS450W. Together, these two substitutions increase E_o by 1084-fold (making it 4.9x10^{-4}) without affecting agonist binding (33, 34).

Statistical analysis

The goodness of fit for the efficiency frequency distribution (Fig. 5A) was done using Prism software (GraphPad Inc., San Diego, CA). The F-test rejects the null hypothesis (Gaussian fit) over sum of two Gaussian with an F-value (F=3.9) and significance (P-value, <0.05). A k-means cluster analysis algorithm (MATLAB®, MathWorks, Natick, MA) was used to define agonist groups for 2D cluster analysis,

efficiency and head-group volume (Fig. 5B). Correlation significance between log EC_{50}, either measured from the CRC or calculated from knowledge of efficiency (Fig. 6A) was performed with Pearson's correlation test using Prism software. The P-value (two-tail) <0.0001 and r^2=0.78 imply that there is a significant correlation.

Agonists. Agonist structures are shown in Figs. 3 and 4. The agonist head-group volumes were calculated using Chimera (35) (Fig. 5B). Cytisine, varenicline, tetraethylammonium and tetramethylphosphonium were from Sigma® (St. Louis, MO). The sources for other agonists are given in previous publications (5, 20).

Acknowledgements: We thank Mary Teeling, Marlene Shero and Janet Jordan for technical assistance. Supported by NS-064969 and GM-121463

Competing interests: The authors declare no competing financial or non-financial interests.

Supplementary Information (SI):

Figure 4–figure supplement 1-3: Interval-duration histograms and example cluster for agonists tested in the study.
Figure 6–Source Data 1: Individual ACh efficiencies of binding site mutations.
Figure 7–Source Data 1: Calculated EC_{50} from P_o^{max}, using η and E_o.
Figure 7–Source Data 2: Calculated unliganded gating (E_o) values from EC_{50} and P_o^{max} using η.

References

1. Gharpure A, Noviello CM, Hibbs RE. Progress in nicotinic receptor structural biology. Neuropharmacology. 2020;171:108086.
2. Nayak TK, Auerbach A. Cyclic activation of endplate acetylcholine receptors. Proc Natl Acad Sci U S A. 2017;114(45):11914-9.
3. Rahman MM, Teng J, Worrell BT, Noviello CM, Lee M, Karlin A, et al. Structure of the Native Muscle-type Nicotinic Receptor and Inhibition by Snake Venom Toxins. Neuron. 2020;106(6):952-62 e5.
4. Colquhoun D. Binding, gating, affinity and efficacy: the interpretation of structure-activity relationships for agonists and of the effects of mutating receptors. Br J Pharmacol. 1998;125(5):924-47.
5. Nayak TK, Vij R, Bruhova I, Shandilya J, Auerbach A. Correction: Efficiency measures the conversion of agonist binding energy into receptor conformational change. J Gen Physiol. 2020;152(1).
6. Vij R, Purohit P, Auerbach A. Modal affinities of endplate acetylcholine receptors caused by loop C mutations. J Gen Physiol. 2015;146(5):375-86.
7. Auerbach A. Dose-Response Analysis When There Is a Correlation between Affinity and Efficacy. Mol Pharmacol. 2016;89(2):297-302.
8. Jadey S, Auerbach A. An integrated catch-and-hold mechanism activates nicotinic acetylcholine receptors. J Gen Physiol. 2012;140(1):17-28.
9. Yehia A, Wei H. Studying Nicotinic Acetylcholine Receptors Using the IonFlux Microfluidic-Based Automated Patch-Clamp System with Continuous Perfusion and Fast Solution Exchange. Curr Protoc Pharmacol. 2020;88(1):e73.
10. Jadey S, Purohit P, Auerbach A. Action of nicotine and analogs on acetylcholine receptors having mutations of transmitter-binding site residue alphaG153. J Gen Physiol. 2013;141(1):95-104.
11. Purohit Y, Grosman C. Estimating binding affinities of the nicotinic receptor for low-efficacy ligands using mixtures of agonists and two-dimensional concentration-response relationships. J Gen Physiol. 2006;127(6):719-35.
12. Tripathy S, Zheng W, Auerbach A. A single molecular distance predicts agonist binding energy in nicotinic receptors. J Gen Physiol. 2019;151(4):452-64.
13. Bruhova I, Gregg T, Auerbach A. Energy for wild-type acetylcholine receptor channel gating from different choline derivatives. Biophys J. 2013;104(3):565-74.
14. Ling HW. Actions of dimethylphenylpiperazinium. Br J Pharmacol Chemother. 1959;14:505-11.
15. Purohit P, Bruhova I, Gupta S, Auerbach A. Catch-and-Hold Activation of Muscle Acetylcholine Receptors Having Transmitter Binding Site Mutations. Biophysical Journal. 2014;107(1):88-99.
16. Jackson MB. Kinetics of unliganded acetylcholine receptor channel gating. Biophys J. 1986;49(3):663-72.
17. Jha A, Auerbach A. Acetylcholine receptor channels activated by a single agonist molecule. Biophys J. 2010;98(9):1840-6.
18. Purohit P, Auerbach A. Unliganded gating of acetylcholine receptor channels. Proc Natl Acad Sci U S A. 2009;106(1):115-20.

19. Nayak TK, Purohit PG, Auerbach A. The intrinsic energy of the gating isomerization of a neuromuscular acetylcholine receptor channel. J Gen Physiol. 2012;139(5):349-58.
20. Bruhova I, Auerbach A. Molecular recognition at cholinergic synapses: acetylcholine versus choline. J Physiol. 2017;595(4):1253-61.
21. Lape R, Colquhoun D, Sivilotti LG. On the nature of partial agonism in the nicotinic receptor superfamily. Nature. 2008;454(7205):722-7.
22. Mukhtasimova N, Lee WY, Wang HL, Sine SM. Detection and trapping of intermediate states priming nicotinic receptor channel opening. Nature. 2009;459(7245):451-4.
23. Gupta S, Chakraborty S, Vij R, Auerbach A. A mechanism for acetylcholine receptor gating based on structure, coupling, phi, and flip. J Gen Physiol. 2017;149(1):85-103.
24. Sauguet L, Shahsavar A, Poitevin F, Huon C, Menny A, Nemecz A, et al. Crystal structures of a pentameric ligand-gated ion channel provide a mechanism for activation. Proc Natl Acad Sci U S A. 2014;111(3):966-71.
25. Purohit P, Mitra A, Auerbach A. A stepwise mechanism for acetylcholine receptor channel gating. Nature. 2007;446(7138):930-3.
26. Mukhtasimova N, Free C, Sine SM. Initial coupling of binding to gating mediated by conserved residues in the muscle nicotinic receptor. J Gen Physiol. 2005;126(1):23-39.
27. Chang Y, Ghansah E, Chen Y, Ye J, Weiss DS. Desensitization mechanism of GABA receptors revealed by single oocyte binding and receptor function. J Neurosci. 2002;22(18):7982-90.
28. Sakmann B, Patlak J, Neher E. Single acetylcholine-activated channels show burst-kinetics in presence of desensitizing concentrations of agonist. Nature. 1980;286(5768):71-3.
29. Nicolai C, Sachs F. Solving ion channel kinetics with the QuB software. Biophysical Reviews and Letters. 2013;8(03n04):191-211.
30. Qin F. Restoration of single-channel currents using the segmental k-means method based on hidden Markov modeling. Biophys J. 2004;86(3):1488-501.
31. Qin F, Auerbach A, Sachs F. Maximum likelihood estimation of aggregated Markov processes. Proc Biol Sci. 1997;264(1380):375-83.
32. Jadey SV, Purohit P, Bruhova I, Gregg TM, Auerbach A. Design and control of acetylcholine receptor conformational change. Proc Natl Acad Sci U S A. 2011;108(11):4328-33.
33. Jha A, Purohit P, Auerbach A. Energy and structure of the M2 helix in acetylcholine receptor-channel gating. Biophys J. 2009;96(10):4075-84.
34. Purohit P, Gupta S, Jadey S, Auerbach A. Functional anatomy of an allosteric protein. Nat Commun. 2013;4:2984.
35. Pettersen EF, Goddard TD, Huang CC, Couch GS, Greenblatt DM, Meng EC, et al. UCSF Chimera--a visualization system for exploratory research and analysis. J Comput Chem. 2004;25(13):1605-12.

Supplementary Information (SI)

Title: Agonist efficiency estimated from concentration-response curves

Abbreviated title: agonist efficiency

Dinesh C. Indurthi and Anthony Auerbach[‡]

Department of Physiology and Biophysics

State University of New York at Buffalo

Buffalo NY 14214

[‡] Corresponding author: auerbach.anthony@gmail.com

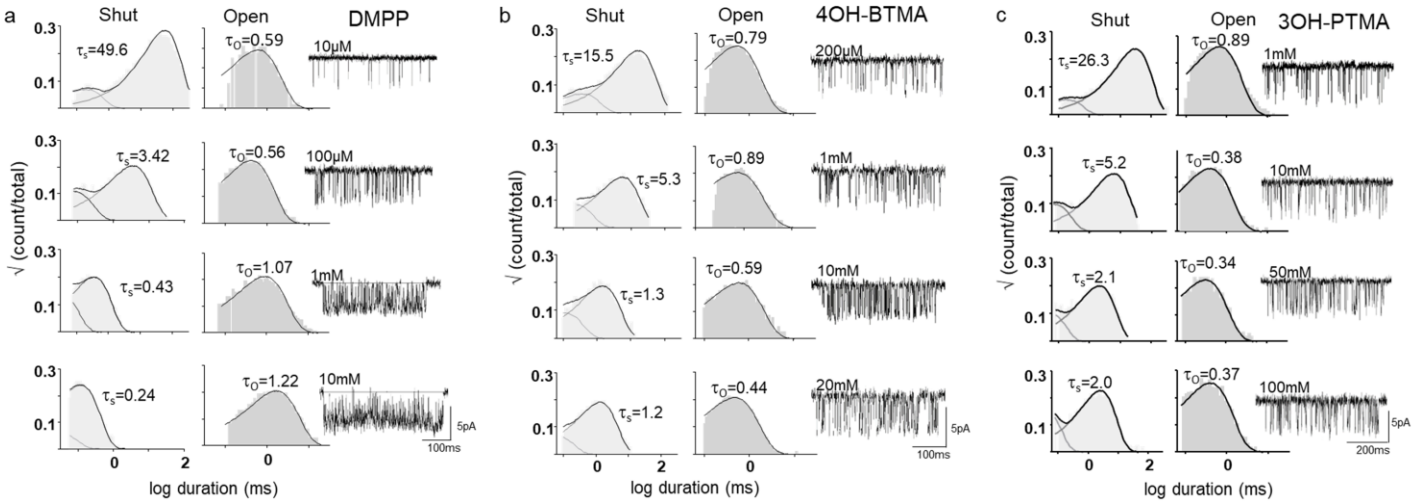

Figure 4 – figure supplement 1. Bind-gate activation of adult-type AChRs in the presence of a. DMPP, dimethylphenylpiperazinium b. 4OH-B, 4-hydroxybutyltrimethylammonium, c. 3OH-P, 3-hydroxypropyltrimethylammonium. Interval-duration histograms and example cluster for each agonist concentration. The predominant intra-cluster shut and open interval durations (τ_s and τ_o, in ms) are noted. O is down; V_m= +70 mV. Background mutation εS450W.

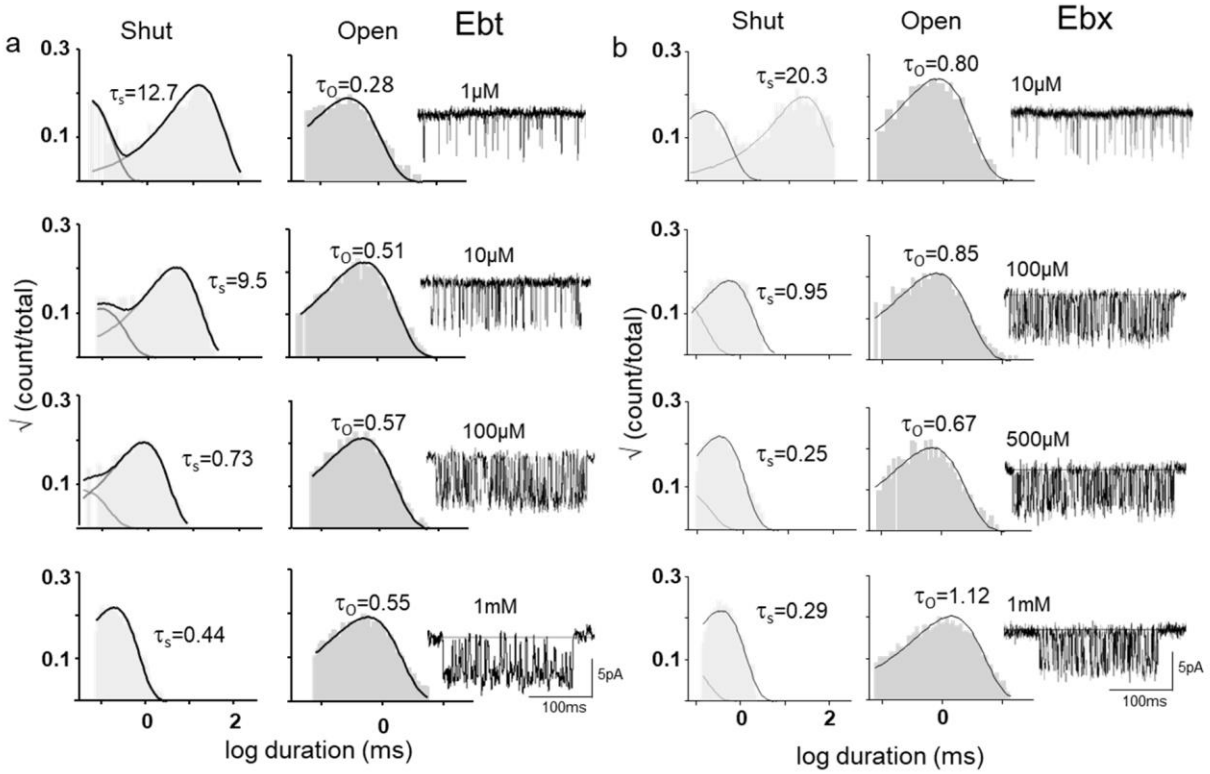

Figure 4 – figure supplement 2. Bind-gate activation of adult-type AChR in the presence of a. Ebt, epibatidine b. Ebx, epiboxidine. Background mutation εS450W.

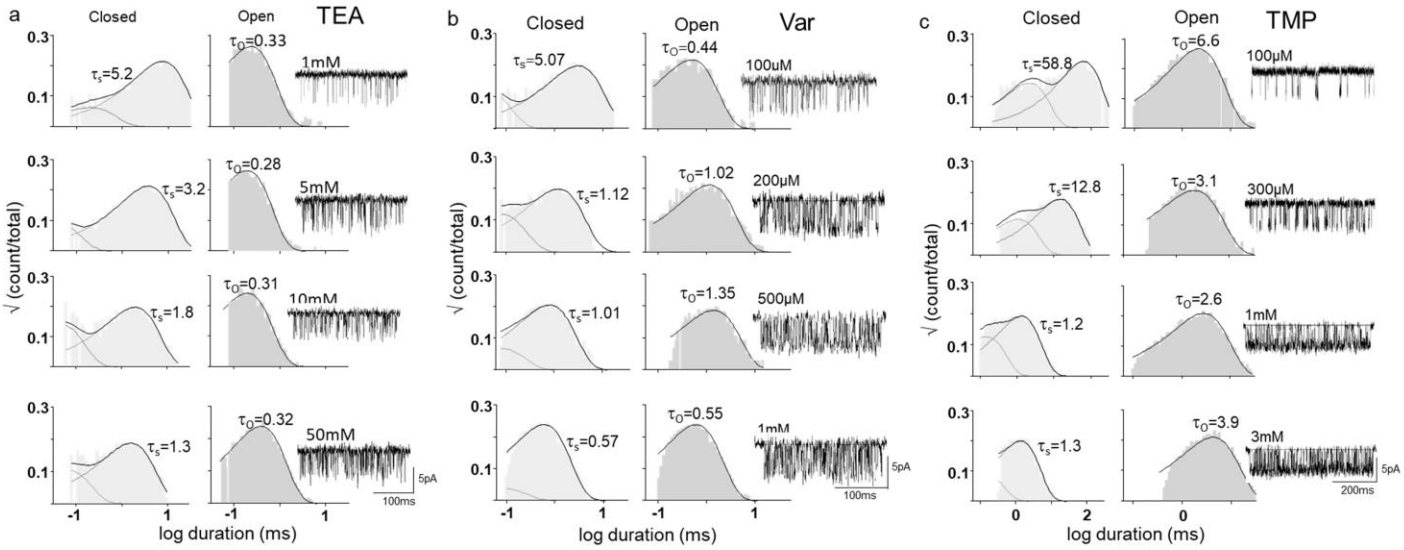

Figure 4 – figure supplement 3. Bind-gate activation of adult-type AChR in the presence of a. TEA, tetraethylammonium, b. Var, varenicline, c. TMP, tetramethylphosphonium. Background mutation εL269F+εE181W.

Figure 6–Source Data 1. efficiency of binding site mutations.

	K_{dC} (mM)	K_{dO} (μM)	Log K_{dC}	Log K_{dO}	κ	η
WT	0.166	0.028	-3.78	-7.55	0.50	*0.50*
αY93W	2.01	1.20	-2.70	-5.92	0.46	*0.54*
H	3.20	2.90	-2.49	-5.54	0.45	*0.55*
A	1.21	1.30	-2.92	-5.89	0.50	*0.50*
F	2.59	5.80	-2.59	-5.24	0.49	*0.51*
S	6.24	14.0	-2.20	-4.85	0.45	*0.55*
αW149Y	2.41	3.00	-2.62	-5.52	0.47	*0.53*
F	12.8	19.0	-1.89	-4.72	0.40	*0.60*
A	28.8	260.0	-1.54	-3.59	0.43	*0.57*
αY190F	3.60	16.0	-2.44	-4.80	0.51	*0.49*
W	6.46	56.0	-2.19	-4.25	0.52	*0.48*
A	16.5	1900	-1.78	-2.72	0.65	*0.35*
αY198F	0.23	0.053	-3.64	-7.28	0.50	*0.50*
H	5.70	9.10	-2.24	-5.04	0.45	*0.55*
W	0.61	0.88	-3.21	-6.06	0.53	*0.47*
S	3.90	12.0	-2.41	-4.92	0.49	*0.51*
T	9.20	38.0	-2.04	-4.42	0.46	*0.54*
L	4.10	21.0	-2.39	-4.68	0.51	*0.49*
A	7.50	41.0	-2.12	-4.39	0.48	*0.52*
εP121L	0.72	2.20	-3.14	-5.66	0.56	*0.44*
Y	1.27	3.00	-2.90	-5.52	0.52	*0.48*
G	1.00	1.20	-3.00	-5.92	0.51	*0.49*

Equilibrium dissociation constant K_d of ACh to closed (C) and open (O) states previously estimated by kinetic modeling (1) for wild-type (wt) and binding site residue mutations in adult-type mouse AChR. Kappa (κ) is the ratio of their binding energies, $\log K_{dC}/\log K_{dO}$ and efficiency (η) is $1-\log K_{dC}/\log K_{dO}$ (1-κ).

Figure 7–Source Data 1. affinity from efficacy, using efficiency.

	Input values		Calculated values			
	P_o^{max}	η	E_2	K_{dC}	EC_{50} (M)	log EC_{50}
ACh	0.96	0.52	23.39	2.94E-04	6.07E-05	-4.22
CCh	0.84	0.52	5.25	5.85E-04	2.52E-04	-3.60
DMP	0.26	0.52	0.35	2.04E-03	2.31E-03	-2.64
DMT	0.42	0.52	0.72	1.46E-03	1.40E-03	-2.85
TMA	0.75	0.52	3.00	7.58E-04	4.24E-04	-3.37
Ana	0.784	0.52	3.63	6.94E-04	3.56E-04	-3.45
Cho	0.049	0.52	0.05	4.94E-03	6.74E-03	-2.17
Nor	0.923	0.52	11.99	4.00E-04	1.15E-04	-3.94
DMPP	0.87	0.52	6.69	5.23E-04	2.01E-04	-3.70
4OH-BTMA	0.29	0.52	0.41	1.90E-03	2.10E-03	-2.68
3OH-PTMA	0.15	0.52	0.18	2.80E-03	3.51E-03	-2.45
Cyt	0.18	0.41	0.22	8.96E-05	1.09E-04	-3.96
Ebx	0.74	0.41	2.85	1.42E-05	8.12E-06	-5.09
Ebt	0.60	0.41	1.50	2.25E-05	1.68E-05	-4.77
Var	0.015	0.41	0.02	6.11E-04	8.55E-04	-3.07
TEA	0.0022	0.41	0.00	2.46E-03	3.47E-03	-2.46
TMP	0.03	0.41	0.03	3.67E-04	5.07E-04	-3.29

Efficacy (P_o^{max}) reported in Table 1 and efficiency (η) from half-maximum (EC_{50}) estimated by calculating the equilibrium dissociation constant to C (K_{dC}) and the di-liganded gating equilibrium constant (E_2) using equations 3, 4 and 6 and an unliganded gating equilibrium constant (E_o) of 5.2×10^{-7}.

Figure 7–Source Data 2. using efficiency to estimate unliganded gating (E_o).

	Input values			Calculated values		
Ligand	EC_{50}	P_O^{max}	η	E_2	K_d	E_0
ACh	4.32E-05	0.96	0.52	23.39024	1.74E-04	1.68E-07
Nor	7.25E-05	0.923	0.52	11.98701	1.99E-04	1.14E-07
CCh	3.20E-04	0.84	0.52	5.25	5.42E-04	4.40E-07
Ana	5.24E-04	0.784	0.52	3.62963	7.19E-04	5.62E-07
TMA	1.20E-03	0.75	0.52	3	1.48E-03	2.23E-06
DMT	4.20E-03	0.42	0.52	0.72	2.73E-03	2.02E-06
DMP	6.70E-03	0.26	0.52	0.351351	3.57E-03	1.75E-06
Cho	4.01E-03	0.049	0.52	0.051525	1.73E-03	5.37E-08
DMPP	2.46E-04	0.87	0.52	6.69	4.79E-04	4.30E-07
4OH-BTMA	2.17E-03	0.29	0.52	0.41	1.20E-03	1.91E-07
3OH-PTMA	3.49E-03	0.15	0.52	0.176471	1.66E-03	1.67E-07
Ebt	3.21E-05	0.60	0.41	1.50	2.79E-05	7.02E-07
Ebx	9.03E-05	0.74	0.41	2.85	1.08E-04	8.79E-06
Cyt	1.37E-04	0.18	0.41	0.219512	6.72E-05	3.49E-07
Var	1.35E-04	0.015	0.41	0.015228	5.66E-05	1.91E-08
TEA	4.20E-03	0.0022	0.41	0.00	1.74E-03	3.23E-07
TMP	6.66E-04	0.03	0.41	0.030928	2.83E-04	3.62E-07

E0 calculated from P_o^{max} and EC_{50} and mean efficiency of the efficiency group they belong (0.52 or 0.41) using Eq. 4 and 3 to calculate E_2 and K_d and Eq. 6 to estimate E_o using efficiency.

Reference:

1. Purohit P, Bruhova I, Gupta S, Auerbach A. Catch-and-Hold Activation of Muscle Acetylcholine Receptors Having Transmitter Binding Site Mutations. Biophysical Journal. 2014;107(1):88-99.